Published in final edited form as:
Adv Healthc Mater. 2012 March ; 1(2): 172–176. doi:10.1002/adhm.201200002.

Microfabrication-Compatible Nanoporous Gold Foams as Biomaterials for Drug Delivery

Erkin Seker,
Department of Electrical and Computer Engineering, University of California, Davis, Davis, CA 95616, USA

Center for Engineering in Medicine, Harvard Medical School & Massachusetts General Hospital, Shriners Hospitals for Children, Boston, MA 02114, USA

Yevgeny Berdichevsky,
Department of Neurology, Harvard Medical School & Massachusetts General Hospital, Boston, MA 02114, USA

Kevin J. Staley, and
Department of Neurology, Harvard Medical School & Massachusetts General Hospital, Boston, MA 02114, USA

Martin L. Yarmush
Center for Engineering in Medicine, Harvard Medical School & Massachusetts General Hospital, Shriners Hospitals for Children, Boston, MA 02114, USA

Department of Biomedical Engineering, Rutgers University, Piscataway, NJ 08854, USA

Keywords

Biomaterials; cell-material interaction; drug delivery; multifunctional coatings; nanoporous materials

There is an unmet need for multi-functional devices that can monitor and modulate biological activity in order to effectively study biological phenomena and systematically develop therapeutics. Even though miniaturization technology has significantly enhanced the capabilities of such devices, increasing demands for multi-functionality within a small device footprint require innovations on the materials front, where nanostructured materials offer unique opportunities.[1–6] Nanoporous gold (np-Au), produced by a self-assembly process involving selective dissolution of silver from a gold-silver alloy,[7] is one such material that has great potential for biomedical applications with its large effective surface area, ease of surface functionalization, and electrical conductivity. However, it has mainly received attention for its catalytic performance[8] and fundamental scientific investigations,[9, 10] while its biomedical applications remain largely unexplored. We have previously shown this material's utility for a biomedical application, where np-Au was used as a multiple electrode array coating, exhibiting increased sensitivity in detecting electrical activity from organotypic hippocampus slices.[11] A desirable attribute for functional biomedical coatings is drug delivery capability to modulate tissue response *in situ*. Np-Au with its controllable open-pore structure is an ideal material for this purpose. The objective

Correspondence to: Erkin Seker.

Supporting Information
Supporting Information is available from the Wiley Online Library or from the author.

of this paper is to illustrate that: (i) np-Au is permissive to culturing adherent cells; and (ii) the porous network can be used for releasing biologically-relevant molecules for controlling cell behavior, which is demonstrated by the delivery of a drug that suppresses cell proliferation. Taken together with np-Au's performance in monitoring electrophysiological activity, the current findings promise an "all-in-one" functional coating that enables biosensing, drug delivery, and biocompatibility.

An important initial performance parameter for a new biomaterial is its capability to sustain cell adhesion. No such demonstration exists for np-Au to the best of our knowledge. Therefore, as a preliminary test of np-Au's biocompatibility, we evaluated the effect of surface morphology and metallurgy on cellular attachment using four different samples: (i) 12 mm-diameter circular plain glass cover slips; (ii) 5 mm-diameter gold spots patterned on the glass cover slips; (iii) 5 mm-diameter np-Au spots patterned on the glass cover slips; and (iv) 5 mm-diameter np-Au spots with a coarser pore morphology. Since gold and glass are well-established biocompatible materials,[12] they served as suitable references for evaluating np-Au biocompatibility. Pore morphologies of the np-Au coating with an interconnected open-pore structure and the np-Au samples with coarser pore morphology (produced by heat treatment at 450°C for 10 minutes[13]) are shown in Figure 1 (bottom row). Thermal treatment produces larger pores, while minimally affecting the characteristic pore structure via thermally-enhanced surface diffusion and pore coalescence mechanisms.[13] The untreated np-Au coatings had a percent porosity of 24.6±1.6 and average pore area of 2786±531 nm^2 (diameter of 59.3±5.8 nm with circular pore approximation). Thermal treatment had a negligible effect on percent porosity; however, it led to an order of magnitude increase in average pore area (23682 ± 2062 nm^2), as shown in Table 1. Film thickness (~294±3 nm) was slightly lower than the 300 nm-thick precursor alloy thickness, due to volumetric contractions during dealloying.[14]

For the cell viability and drug-release experiments, we used murine astrocyte cell lines. The cells were seeded onto the four different samples (i.e., glass, gold, and both untreated and heat-treated np-Au) at a density of ~25,000 cells/cm^2. One day after cell seeding, the cells were stained to capture fluorescent images of the f-actin cytoskeleton and nucleus, and imaged with an epifluorescent microscope. Images were digitally processed to quantify percent cell coverage (i.e., percent area covered by cells), average cell area, and cell density (i.e., number of cells per unit area) in each image (Table 1).

A set of cells grown on the different surfaces was prepared for scanning electron microscopy (SEM) studies to observe the cell-surface interactions. Figure 1 illustrates representative images of astrocytes cultured on glass, gold, and np-Au surfaces, as well as the high-magnification SEM images of different surfaces. Cells on np-Au surfaces appeared to have shorter processes (untreated: 6.9 ± 3.3 μm and heat-treated: 6.1 ± 3.4 μm) compared to those of cells on non-porous surfaces (glass: 11.8 ± 3.7 μm and gold: 16.6 ± 7.0 μm). It is possible that the porous surface allows for "mechanical anchoring", that is, cellular processes to latch into nanopits providing additional stability over "biochemical anchoring" due to focal adhesions. While the cell density on different surfaces was not statistically different (single-variable ANOVA p=0.6), average cell size was slightly bigger on gold and glass surfaces compared to nanoporous gold surfaces (Table 1). One reason for this may be that np-Au surfaces with nanopits likely accommodate a limited number of focal adhesions compared to those by a non-porous gold surface, thereby reducing cellular spreading. This was supported by the observation that over-confluent astrocyte layers delaminated due to in-plane stress arising from cell-cell tensile interactions. It is important to note that the heat-treated np-Au sample with much larger pores (but similar percent porosity) did not lead to a significant difference in average cell area compared to the untreated np-Au. It is plausible that there need to be much larger changes in pore morphology (such as both bigger and smaller pores

than tested here) to significantly modify cellular adhesion. The important conclusion of the comparative cell adhesion experiments is that np-Au performs equally well as the commonly-used materials (i.e., glass and gold) in microdevices.[12] Other cell types (i.e., primary murine cortical neurons and human fibroblasts, microglia, and endothelial cells) were also viable on np-Au (see Figure S1). We tested the biocompatibility of np-Au further by culturing organotypic hippocampus slices on an array of np-Au spots. Organotypic slices have been shown to provide a physiologically relevant model, as they preserve the cytoarchitecture of the brain[15, 16] and provided a means to evaluate biocompatibility of np-Au. For this, we cultured organotypic slices over an array of microfabricated 30 μm-diameter np-Au spots for 12 days, at which point they were stained to visualize healthy neurons in the slice. The np-Au microspot array had identical film properties to that of the 5 mm-diameter spots used for the astrocyte culture. Figure 2 shows that organotypic hippocampus slices remained viable on np-Au spot arrays, retaining intact neural layers stained in green.

Many biomedical devices (e.g., neural electrodes[17] and vascular stents[18]) require the capability for *in situ* drug delivery to modulate physiological response. One such scenario is the release of pharmaceuticals to suppress the proliferation of reactive cells that negatively impact device performance (e.g., astrocytic gliosis in response to implanted neural electrodes[17]). For this, it would be highly useful to have an electrically conductive biomaterial that can monitor electrophysiological activity, as well as simultaneously modulate surrounding tissue response by *in situ* drug delivery. Np-Au, with its large surface area, is a promising material for such purpose. In order to test the capability of np-Au coatings for sustained molecular release, we monitored the release of fluorescent molecules from np-Au coatings over time using fluorescein as a model molecule. Np-Au coatings retained and released fluorescent molecules unlike compact surfaces. The sustained release from np-Au is likely due to the large specific surface area resulting in a large number of surface-molecule interactions along the pore walls as the molecules diffuse out of the porous network (Figure 3). While molecular release from a porous coating does not lead to high concentrations in a large volume, it is probable that the effective concentration that the cells are exposed to at the interface would be much larger than the bulk volume.

The molecular release experiment was subsequently repeated with an anti-mitotic drug cocktail to evaluate the performance of drug release from np-Au coatings in suppressing cellular proliferation. Plain glass cover slips and slips with np-Au spots were loaded with the drug cocktail at different concentrations, washed, and then astrocytes were seeded onto the samples at a density of ~13,000 cells/cm^2. The anti-mitotic drug cocktail included an active ingredient (Ara-C) which is incorporated into the DNA to stop cell proliferation by disrupting DNA synthesis[19, 20]. Two types of controls were employed: (i) non-porous glass cover slips and (ii) np-Au samples loaded with Hank's buffered salt solution (HBSS), which is the vehicle in the drug cocktail. The percent growth on days 1 and 2 were determined by quantifying the cell density on each day for different conditions. Cells continually proliferated on blank glass cover slips regardless of their treatment with anti-mitotic drugs, suggesting that possible physio-adsorption of drug molecules on the glass surface is not sufficient to modulate cell behavior. The np-Au sample treated with the vehicle also exhibited continuous cell proliferation, suggestive of np-Au's biocompatibility. However, np-Au cells treated with the anti-mitotic drug cocktail reduced cellular growth in a dose-dependent manner (Figure 4), suggesting that drug release from the porous network was responsible for suppressing cell proliferation, even though the release rates of individual drug cocktail components may be different. Two different comparisons were performed to statistically confirm this observation, as outlined in Table 2: (i) day-wise comparison of cell proliferation on drug-loaded np-Au samples (i.e., 5X and 50X) to the vehicle; and (ii) day-wise comparison of cell proliferation on np-Au samples to the blank glass cover slips treated

with the two extreme conditions (i.e., vehicle and 50X). Fluorescein release from np-Au samples (Figure 3) exhibit significantly smaller standard deviations compared to those for cell proliferation (Figure 4). This suggests that the molecular release and/or preceding drug loading are consistent from sample to sample. It is therefore probable that the large standard deviations in Figure 4 are due to inherent variability of cell growth.

In this study, we compared the morphological response of astrocytes to various materials and demonstrated that drug release from np-Au coatings can modulate cellular proliferation. An important characteristic of new materials is the ease of integration with existing technologies. As np-Au can be deposited and micropatterned using conventional microfabrication techniques, it can be readily incorporated into microdevices, potentially creating new device capabilities. Np-Au performed comparably well to other samples typically used for cell culture in sustaining adherent cell proliferation, suggesting biocompatibility. The long-term (~2 weeks) viability of an organotypic tissue slice on np-Au spot array provided an additional confirmation of np-Au's promise as a biocompatible material. Np-Au samples had the capability to retain and release drugs, as demonstrated by the cellular suppression in response to anti-mitotic drugs delivered from the nanoporous structure. The porous surfaces appeared to be minimally fouled by exposure to cells and culture media, as judged by the unobstructed surface pore structure, which is important for sustained drug delivery. In addition, as differences in pore morphology did not produce significant effects in cellular response, pore morphology may be modulated to adjust molecular release profile while not affecting biological response. Additional studies, particularly in *in vivo* models to evaluate np-Au's biocompatibility and its interaction with glial cells as well as mechanistic studies to understand drug release patterns as a function of pore morphology and molecular properties are currently underway to comprehensively evaluate np-Au as a multifunctional material. A np-Au coating can potentially be applied to surfaces with engineered microtopographies, where the nanoporous network is responsible for drug delivery, while the microtopography dictates cellular attachment, migration, and other cellular functions.[21, 22] These features, taken together with its biosensor applications,[11] confirm the utility of np-Au as a valuable multi-functional biomedical device coating.

Experimental Section

Details of the sample preparation, cell culture, drug delivery, and imaging can be found in Supporting Information.

Sample fabrication and characterization

The gold spots were deposited by direct-current sputtering (AJA Sputtering Instrument) of 15 nm-thick chrome for adhesion and 200 nm-thick gold under 4 mTorr argon ambience. Gold-silver alloy spots (precursor to np-Au synthesis) were produced by sputtering 15 nm-thick chrome adhesion layer, 50 nm-thick gold seed layer, and 300 nm-thick gold-silver alloy (30% gold and 70% silver; atomic %). The array of 30 μm-diameter np-Au spots with 200 μm center-to-center spacing on 12 mm×24 mm glass cover slips were fabricated via lift-off process. The final np-Au structure was batch-fabricated by immersing the AuAg samples in nitric acid (65%) at 50°C. The samples were rinsed in deionized (DI) water and stored in DI water for a week while changing the liquid every other day. In order to produce np-Au surfaces with coarser pore morphology, some np-Au samples were heat-treated in a rapid thermal annealer (Modular Process Technology), as thermal exposure generally coarsens np-Au morphology.[13] The coatings were imaged with a scanning electron microscope (SEM; Zeiss Ultra55) and pore structures were analyzed using a custom ImageJ (National Institutes of Health shareware) macro.

Cell culture and imaging

The murine astrocytes were received Prof. Bradley Hyman at Massachusetts General Hospital. The culture media composition was: 10% heat-inactivated fetal bovine serum (Sigma), 0.2% Geneticin antibiotic as received (Invitrogen), 1X GlutaMAX (Invitrogen), and DMEM Advanced (Invitrogen) as the basal medium. Cell cultures were maintained in a humidified incubator at 37°C and 5% CO_2. For cellular quantification, the cells were fixed with 4% paraformaldehyde in phosphate buffered saline (PBS), stained using phalloidin (conjugated with Alexa 488 fluorophore, Invitrogen) to visualize f-actin cytoskeleton, and counterstained with DAPI to visualize cell nuclei using an epifluorescent microscope (Zeiss Axiovert). For SEM studies, the cells were fixed with 2.5% glutaraldehyde, dehydrated in graded ethanol solutions and hexamethyldisilazane (Sigma), coated with a thin layer of gold, and imaged with a SEM (Zeiss Ultra55) at various magnifications. Both fluorescent and SEM images were analyzed using an ImageJ macro to determine cell counts, average cell areas, and cellular process lengths.

Organotypic hippocampus slice preparation and imaging

350 μm-thick hippocampus slices from postnatal day 7 Sprague-Dawley rat pups were dissected as described previously.[11] The experiments were conducted per the approval of the Massachusetts General Hospital Subcommittee on Research Animal Care. On day-in-vitro (DIV) 12, the slices were fixed and stained with SYTO 10 (Invitrogen), which leads to a Nissl-like staining of healthy neurons.

Molecular release experiment

For fluorescein release experiment, 12 mm^2 ~300 nm-thick np-Au coatings patterned on silicon chips were loaded with 10 mM fluorescein solution over night, rinsed in DI water, and immersed in 250 μL tubes of DI water. The immersion solution was sampled to spectroscopically determine the amount of released fluorescein over time using a fluorospectrometer (Nanodrop, Thermo Scientific).

Drug delivery experiment

The stock solution (5000X) of the anti-mitotic drug cocktail consisted of 160 mg of cytosine-β-D-arabino-funanoside (Ara-C) (Sigma), 160 mg of uridine (Sigma), and 160 mg of 5-Fluro-2’-deoxyuridine (Sigma) in 40 mL of Hank’s buffered salt solution (HBSS). The blank glass and 5 mm-diameter np-Au spots were treated with 5X and 50X working solutions (by immersion for approximately five hours), and astrocytes were cultured on the samples for two days. On days 1 and 2 after cell seeding, the cells were stained, imaged, and counted as described before. The cell density on cover slips (blank glass cover slips and np-Au spot-patterned cover slips) for each condition were normalized to the cell density on the day of seeding (Day 0) for the cover slips that were loaded only with the vehicle (blank glass cover slips and np-Au spot-patterned cover slips respectively).

Acknowledgments

ES acknowledges support by Massachusetts General Hospital (MGH) Fund for Medical Discovery award 217035, facilities at Harvard University – Center for Nanoscale Systems, and start-up funds from University of California, Davis – College of Engineering. MLY acknowledges support by National Institutes of Health (NIH) awards AI063795 and EB002503. We acknowledge the help of Dr. Gavrielle Price (MGH) with endothelial cell culture, Dr. Hansang Cho (MGH) with microglia culture, and Dr. Eloise Hudry (MGH) with cortical neuron culture.

References

1. Roco MC. Curr. Opin. Biotechnol. 2003; 14:337. [PubMed: 12849790]

2. Gultepe E, Nagesha D, Sridhar S, Amiji M. Advanced drug delivery reviews. 2010; 62:305. [PubMed: 19922749]
3. Kotov N, Winter J, Clements I, Jan E, Timko B, Campidelli S, Pathak S, Mazzatenta A, Lieber C, Prato M. Adv. Mater. 2009; 21:3970.
4. Patolsky F, Timko B, Yu G, Fang Y, Greytak A, Zheng G, Lieber C. Science. 2006; 313:1100. [PubMed: 16931757]
5. Cheng MMC, Cuda G, Bunimovich YL, Gaspari M, Heath JR, Hill HD, Mirkin CA, Nijdam AJ, Terracciano R, Thundat T. Curr. Opin. Chem. Biol. 2006; 10:11. [PubMed: 16418011]
6. Mark D, Haeberle S, Roth G, Von Stetten F, Zengerle R. Chem. Soc. Rev. 39:1153. [PubMed: 20179830]
7. Erlebacher J, Aziz M, Karma A, Dimitrov N, Sieradzki K. Nature. 2001; 410:450. [PubMed: 11260708]
8. Snyder J, Fujita T, Chen M, Erlebacher J. Nature Materials. 2010; 9:904.
9. Jin HJ, Weissmüller J. Science. 2011; 332:1179. [PubMed: 21636769]
10. Biener M, Biener J, Wichmann A, Wittstock A, Baumann TF, B umer M, Hamza A. Nano Lett. 2011; 11:3085. [PubMed: 21732623]
11. Seker E, Berdichevsky Y, Begley M, Reed M, Staley K, Yarmush M. Nanotechnology. 2010; 21:125504. [PubMed: 20203356]
12. Voskerician G, Shive MS, Shawgo RS, Recum H, Anderson JM, Cima MJ, Langer R. Biomaterials. 2003; 24:1959. [PubMed: 12615486]
13. Seker E, Gaskins J, Bart-Smith H, Zhu J, Reed M, Zangari G, Kelly R, Begley M. Acta Mater. 2007; 55:4593.
14. Parida S, Kramer D, Volkert C, Rösner H, Erlebacher J, Weissmüller J. Phys. Rev. Lett. 2006; 97:35504.
15. Gähwiler B, Capogna M, Debanne D, McKinney R, Thompson S. Trends in Neurosciences. 1997; 20:471. [PubMed: 9347615]
16. Yu Z, McKnight TE, Ericson MN, Melechko AV, Simpson ML, Morrison B III. Nano Lett. 2007; 7:2188. [PubMed: 17604402]
17. Polikov VS, Tresco PA, Reichert WM. J Neurosci Methods. 2005; 148:1. [PubMed: 16198003]
18. Fattori R, Piva T. The Lancet. 2003; 361:247.
19. Dyhrfjeld-Johnsen J, Berdichevsky Y, Swiercz W, Sabolek H, Staley K. Journal of Clinical Neurophysiology. 2010; 27:418. [PubMed: 21076333]
20. Billingsley M, Mandel H. J. Pharmacol. Exp. Ther. 1982; 222:765. [PubMed: 7108773]
21. Stevens MM, George JH. Science. 2005; 310:1135. [PubMed: 16293749]
22. Ochsner M, Textor M, Vogel V, Smith ML. PloS one. 2010; 5:e9445. [PubMed: 20351781]

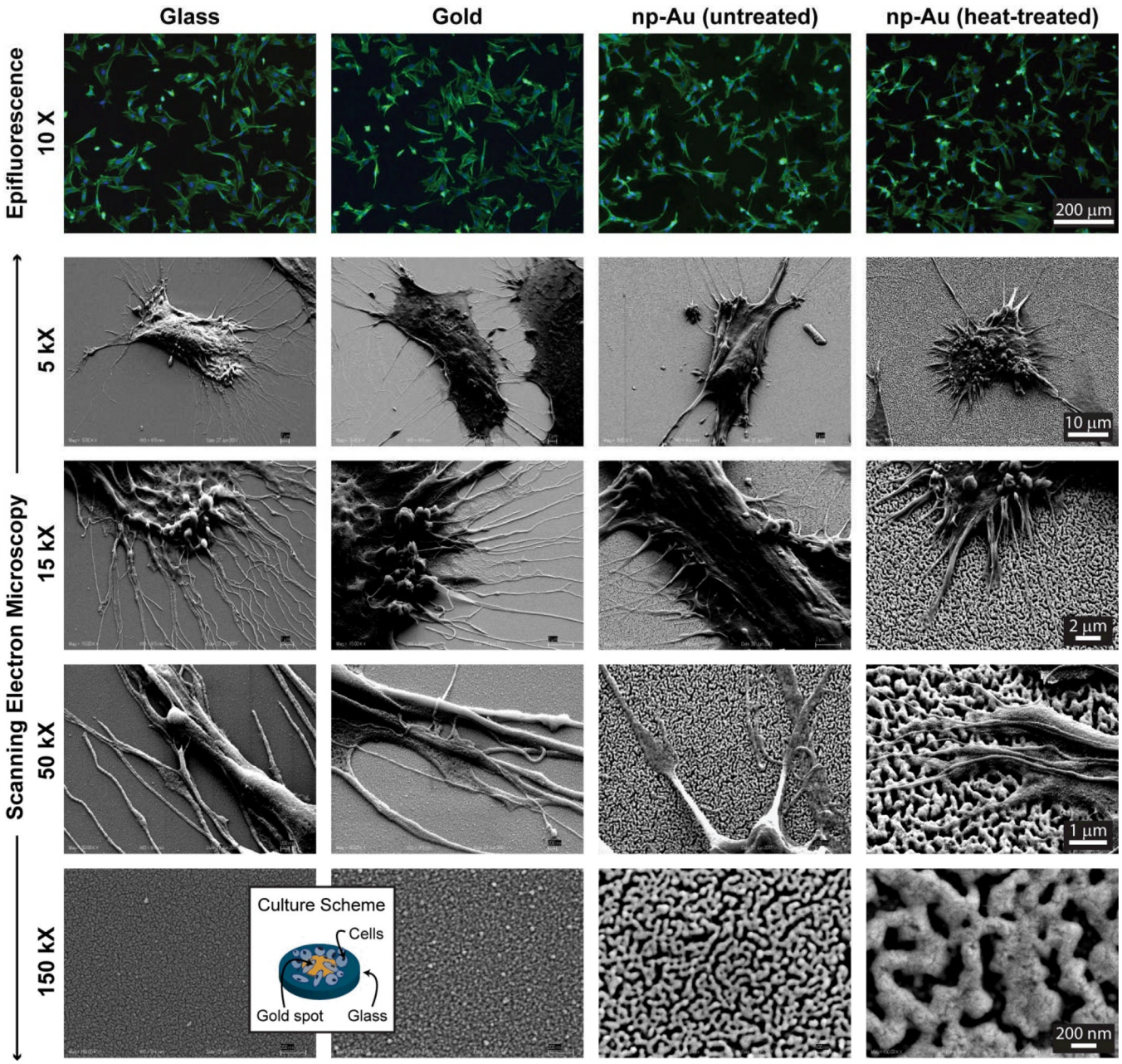

Figure 1.

Epifluorescent and scanning electron microscope images of astrocytes on glass, gold, and np-Au samples (f-actin: green, nucleus: blue). The bottom row displays the high-magnification morphology of different surfaces. The average pore area for untreated and heat-treated np-Au coatings are 2786 ± 531 nm^2 and 23682 ± 2062 nm^2 respectively. The inset illustrates the cell culture scheme. Magnifications are the same across individual rows. Np-Au surfaces are permissive to cell proliferation, similar to commonly used materials like gold and glass surfaces, suggesting np-Au's biocompatibility.

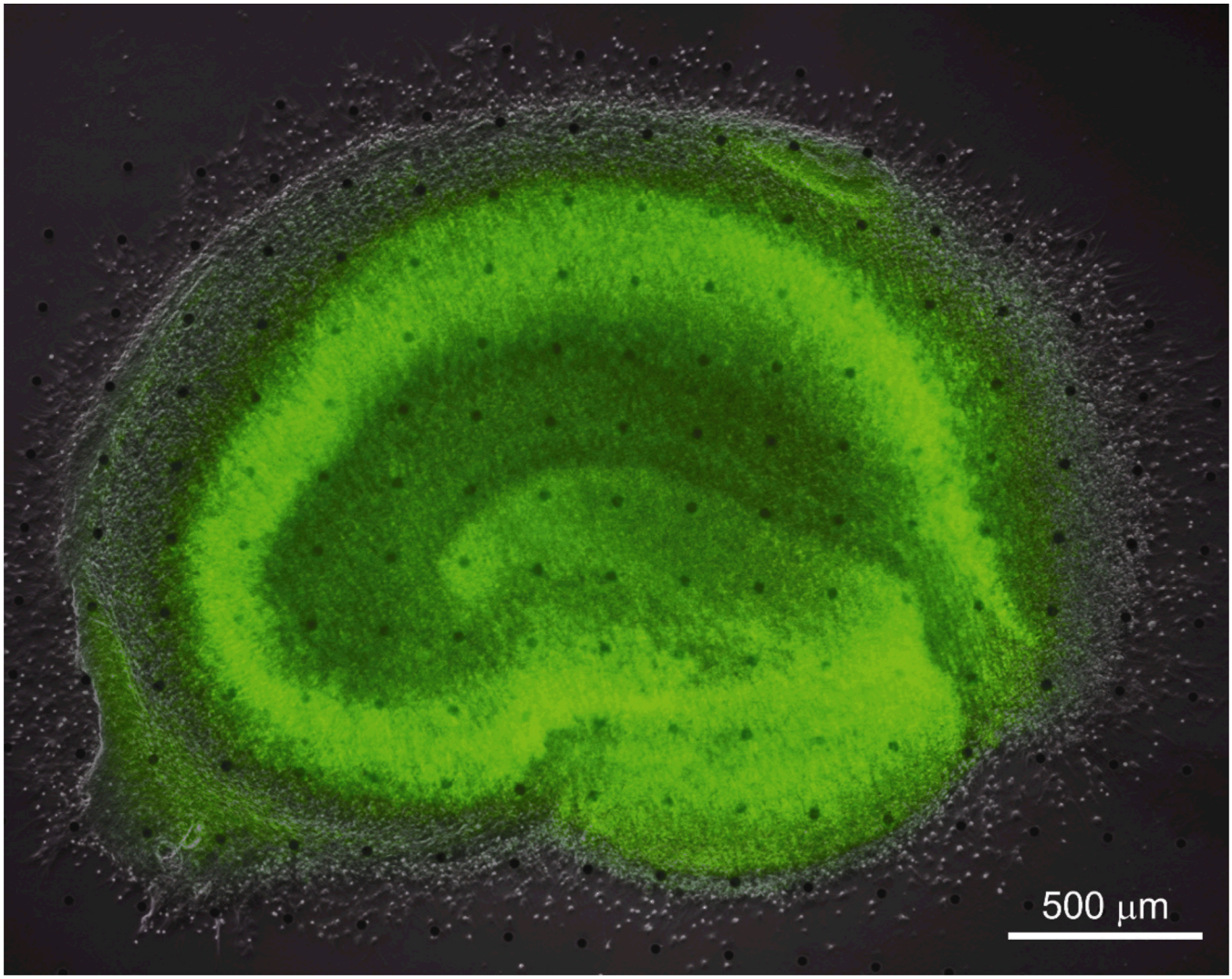

Figure 2.
Well-defined neuronal layers (green SYTO 10-staining) in the bright-field & fluorescent composite image suggest that np-Au does not affect neuronal health. Micro np-Au spots are visible in the background.

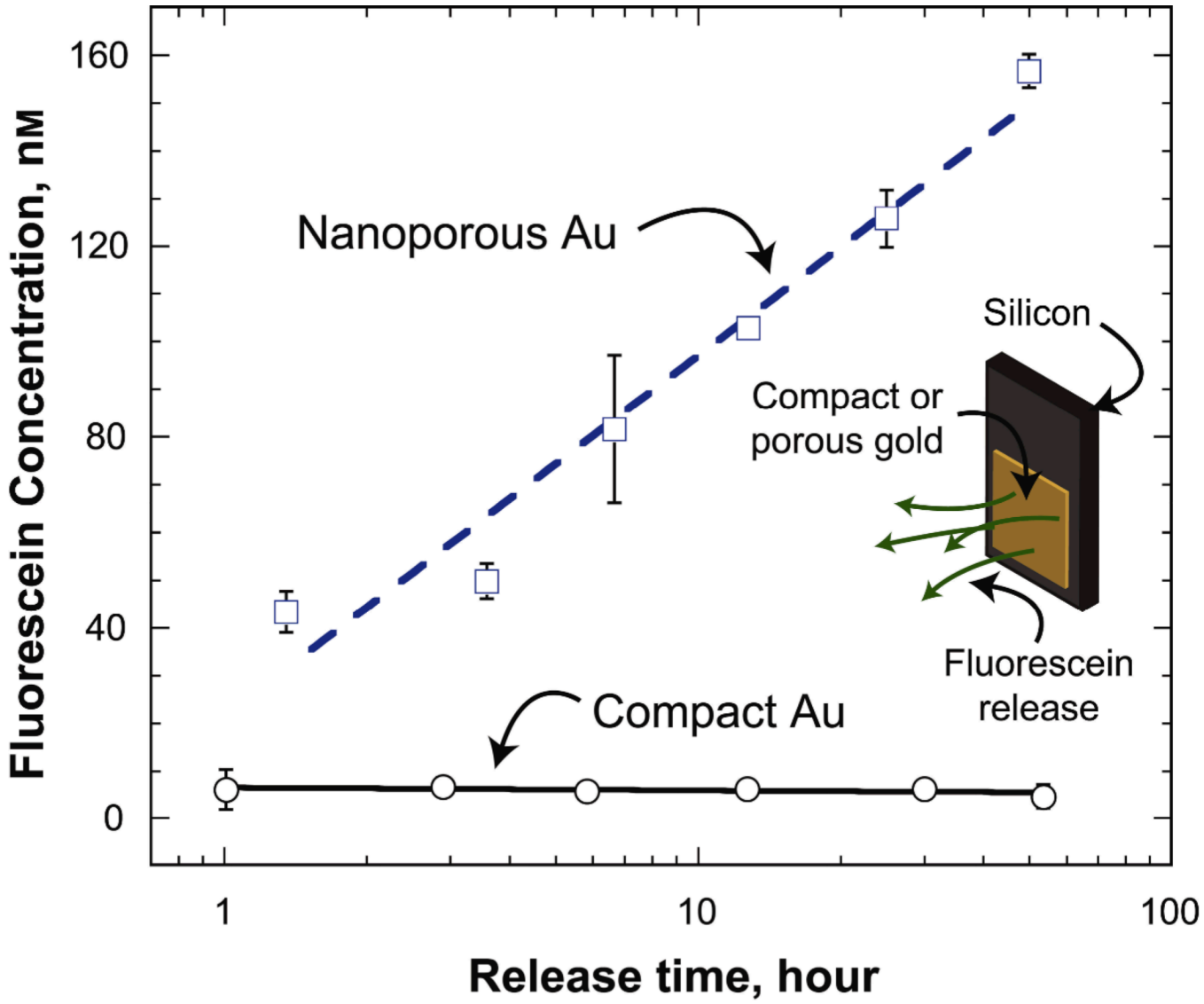

Figure 3.
Fluorescein concentration in the 250 μL-vial increases due to the release of fluorescein molecules from np-Au coatings, but not from compact Au. Error bars show standard deviation of the measurements.

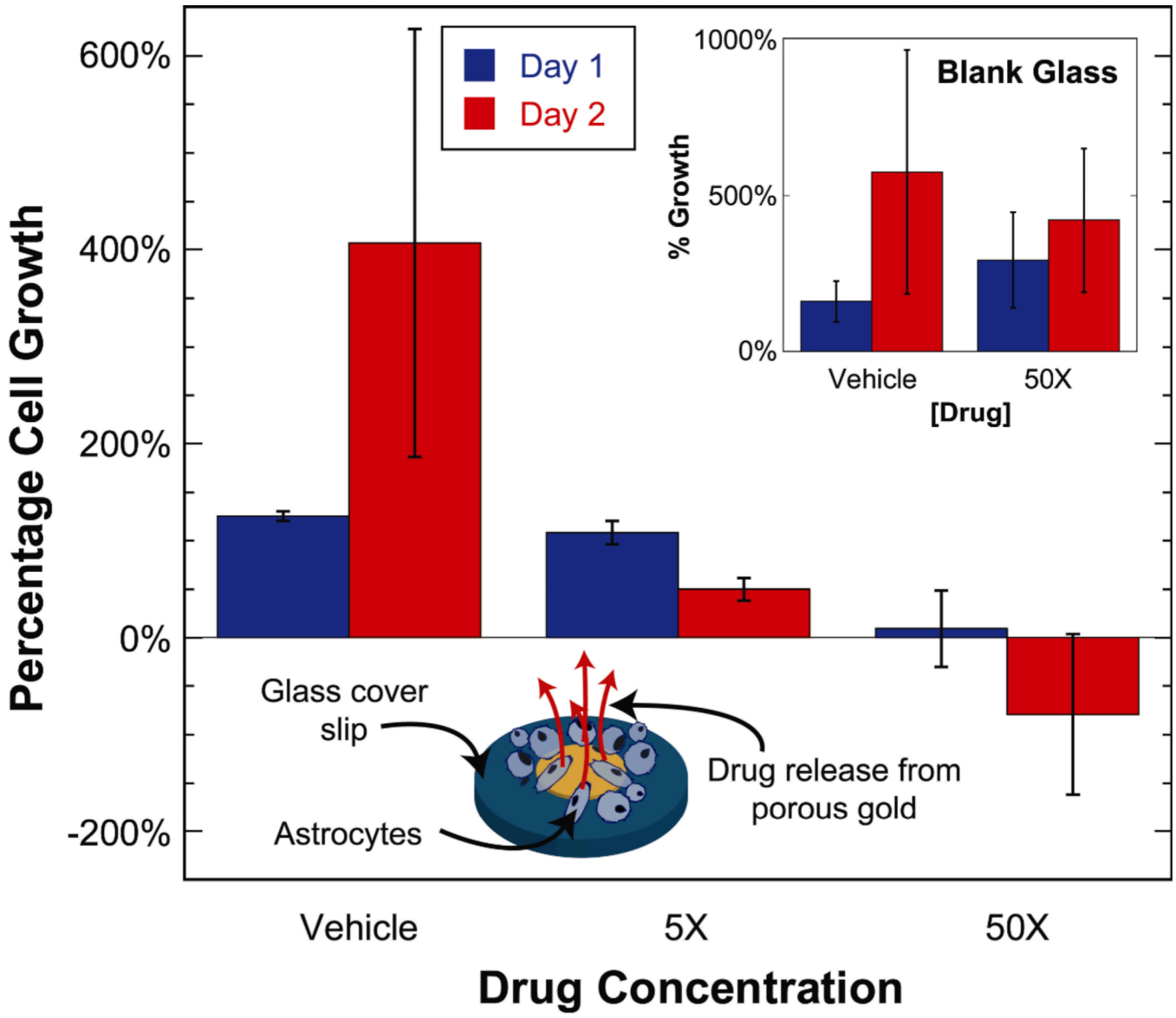

Figure 4.

Astrocyte proliferation on np-Au spots (normalized to cell density on day 0 for samples treated with the vehicle solution) decreased in a dose-dependent manner for days 1 and 2 due to anti-mitotic drug release from np-Au samples. Inset: astrocyte proliferation (normalized to cell density on day 0 for vehicle treatment) on blank glass cover slips treated with the vehicle and 50X concentration of the anti-mitotic drug cocktail. Negative percentage growth values indicate a reduction in cell density with time. Error bars show standard deviation of the measurements.

Table 1

Summary of properties of different samples and quantification of cellular attachment. Student's t-test comparison to untreated np-Au.

Surface	% Average Porosity	Average Pore Area [nm^2]	% Average Cell Coverage	Average Cell Area [μm^2]	Average Cell Density [mm^{-2}]
Glass	-	-	26.7 ± 9.7	1191 ± 260 **	104 ± 24
Gold	-	-	39.7 ± 7.0 *	1457 ± 116 **	119 ± 28
np-Au (untreated)	24.6 ± 1.6	2786 ± 531	19.6 ± 4.9	855 ± 101	100 ± 24
np-Au (heat-treated)	25.1 ± 0.3	23682 ± 2062 ***	23.1 ± 4.0	914 ± 65	110 ± 19

Statistical significance in comparison to untreated np-Au:

* $p<0.001$ (n=20);

** $p<0.005$ (n=20);

*** $p<0.002$ (n=6)

Table 2

Student's t-test p-values for comparing cellular proliferation within np-Au samples and np-Au samples to blank glass cover slips. Drug release from np-Au samples reduced cell proliferation in a dose-dependent manner. Difference was deemed statistically significant for $p < 0.01$.

[Drug]	*Compared to np-Au (vehicle)*		*Compared to blank glass*	
	Day 1	**Day2**	**Day 1**	**Day 2**
Vehicle	-	-	0.116	0.256
5X	7.455×10^{-4}	8.786×10^{-5}	-	-
50X	5.574×10^{-8}	1.055×10^{-6}	2.834×10^{-5}	6.059×10^{-6}